RSC Advances

ROYAL SOCIETY OF CHEMISTRY

www.rsc.org/advances

Biophysical Insight into the Interaction of the Bioflavonoid Kaempferol with Triple and Double Helical RNA and Dual Fluorescence Behaviour of Kaempferol

Lucy Haque, Sutanwi Bhuiya, Richa Tiwari, Ankur Bikash Pradhan and Suman Das*

Department of Chemistry

Jadavpur University

Raja S. C. Mullick Road, Jadavpur

Kolkata 700 032

India

* To whom all correspondence should be addressed.

Tel.: +91 94 3437 3164, +91033 2457 2349

Fax: +91 33 2414 6266

E-mail:

SD: sumandas10@yahoo.com

LH: lucy.haque@gmail.com

SB: s.bhuiya12@gmail.com

RT: tiwariricha1992@gmail.com

ABP: ankurpradhan727@gmail.com

ABSTRACT

The interaction of naturally occurring flavonoid, kaempferol (KMP) with single, double and triple helical forms of RNA has been investigated by different spectroscopic and viscometric techniques. It was found that KMP binds with triple helical [poly(U).poly(A)*poly(U), hereafter U.A*U, dot represents the Watson-Crick and asterisk represents Hoogsteen base pairing respectively] and double helical [poly(A).poly(U), hereafter A.U] forms of RNA, whereas no interaction was observed with single stranded polyuridylic acid [poly-U] under identical experimental conditions. The binding of KMP was found to be stronger with U.A*U ($20 \times 10^4\ M^{-1}$) compared to that of the parent duplex A.U ($9.5 \times 10^4\ M^{-1}$). From Stern-Volmer quenching constant, viscosity measurement and perturbation of CD spectra of RNA revealed that KMP binds to U.A*U structure by intercalation while partial intercalation has been proposed for the binding to duplex RNA structure. Thermodynamic data obtained from temperature dependence study showed that the association was favoured by negative enthalpy and positive entropy changes. Experimental observations indicated that KMP binds and stabilizes the RNA-triplex more than its parent duplex counterpart.

KEYWORDS: Flavonoids; Triplex; Intercalation; Viscometry; Thermodynamics.

Introduction

The novel discovery of double helical structures of DNA in the year of 1953 by Watson and Crick[1] inspired other researchers to investigate other polymorphic structures of nucleic acids.[2,3] The discovery led to an explosion of developments in numerous areas of biochemistry and genetics. In addition to the discovery of B-DNA, a number of alternative canonical and non-canonical forms of DNA/RNA have also been described by several researchers.[4-9] From the very beginning of the discovery, DNA is the pharmacological target of many therapeutic agents and is of great significance for synthesizing new DNA targeted compounds of medicinal use. The interaction of small molecules with DNA is the most promising area of modern research associated with pharmaceutical development processes. Instead of targeting the usual DNA duplex structures, it's higher ordered structures, like triplexes and quadruplexes, serve as convincing targets for therapeutic agents which are very useful in designing various clinical drugs.[9,10] In this context, interaction study of neomycin, an aminiglycoside with higher ordered DNA structures was studied in a great extent by Arya *et. al* .[11,12,13] Along with DNA, the study of single stranded RNAs has been stimulated by the recognition of their potential biological role and genetic applications. Depending upon the environmental conditions RNA can adopt different conformations. The ability of RNA to form secondary or tertiary motif helps it to perform many biological functions *in vivo*.[14,15] Apart from single stranded RNA, triple helical forms of RNA is an important tertiary motif that is found in many pseudoknot and other structured RNAs. Triplex formation has continued to garner much interest in the scientific community because of the possible applications in developing new molecular biology tools. Naturally occurring triplexes are important for shaping RNAs into complex three-dimensional architectures and for diverse biological roles.[15,16] Moreover, triple helical structure in the conserved pseudoknot domain of the telomerase-associated RNA is essential for telomerase activity.[17] The SAM-II riboswitch forms a triple helix that creates a highly specific binding pocket for S-adenosylmethionine.[17] These diverse biological roles of RNA-triplex make it as an important target of many small

molecules of medicinal value. The biological importance of triple helical nucleic acid as well as its different mode of interaction have been described by Arya and his co-authors in their earlier reports.[18,19] RNA-triplex garners much more importance over DNA-triplex now a days. Triple helical structures of RNA is formed by sequence specific binding of a triplex forming oligonucleotide (TFO) in the major groove of a homopyrimidine-homopurine stretch in duplex RNA.[20] Importantly, it permits the single-stranded nucleic acid (RNA) to bind the targeted duplex structure without requiring it to unwind. This unique ability has considerable biotechnological potential and has been extensively studied for use in such applications as modulation of transcription and site-directed recombination.[21,22] The stability of RNA-triplex is basically weaker than their parent duplex. Poor stability of triplex leads its limitations in their applications *in vivo*.[23] One of the remarkable features of triplex is that on binding with small molecules, stability is enhanced in many cases.[9,24,25] Design and development of RNA targeted small molecules is a challenging venture in the present scientific scenario. Among the various RNA-binding small molecules, natural products are considered to be the most valuable clinical agents for their high abundance and low toxicity.

Flavonoids, an important class of natural products, are abundant in fruits and vegetables known to have many beneficial health effects and wide-ranging biological properties. They are well known for taking part in the activities of many enzymes, such as calcium phospholipid-dependent protein kinase, tyrosine protein kinase, phosphorylase kinase and DNA topoisomerase.[26] Nowaday's dietary flavonoids are receiving increasing attention as potential protectors against a variety of human diseases, particularly in cardiovascular and cancer diseases. A large number of mechanisms have been attributed to flavonoids on their antioxidant properties and effects on gene expression. There is an inverse relation between the nutritional effects on human health of flavonoids and the occurrence of several chronic diseases and cancers.[27] The biological activities are mostly ascribed to their notable antioxidant properties as well as their inhibition of several enzymes in the human body.

Antioxidant properties of flavonoids mainly impart its ability to scavenge free radicals and chelate metal ions[28,29] as well as display anti-allergic,[30] anti-inflammatory,[31] anti-microbial[32] and anti-cancer[33] activities. Wide range of biological activities of flavonoids makes them as significant molecular target of various nucleic acids.

The interactions of flavonoids with various nucleic acid structures are playing important role in mechanism of their ascribed actions. The non covalent interactions between several flavonoids and various conformations of nucleic acid have been reported.[34-41] But the interaction study of Kaempferol (3,5,7-trihydroxy-2-(40-hydroxyphenyl)-4H-1-chromen-4-one, hereafter KMP) (Fig. 1) is really scanty till date. KMP, a member of flavonols, is richly found in tea, broccoli, apples, strawberries and beans. It has various biological effects and its effect has been ascribed to its actions as antioxidants, enzyme inhibitors and cell cycle regulators under various conditions.[42,43] According to Kanakis *et al.* the presence of an ortho-hydroxyl group on the B-ring of the flavonoid molecule, number of free hydroxyl groups, a C2–C3 double bond in the C-ring and the presence of a 3-hydroxyl group are the conditions of antioxidant and antiradical activities of flavonoids.[44] Recently Jurasekova *et al*. have also supported the above criteria.[45] Among the different class of flavonoids, KMP, a common component of the human diet, is less characterized. The purpose of the present work is to characterize the binding of KMP with RNA triplex and evaluation of structural properties of KMP on its RNA binding properties. For a comparison purpose we have also studied the interaction of KMP with the double helical counterpart as well as single stranded RNA. Our work is concerned with the spectroscopic and thermodynamic investigation of the interaction of KMP with three different forms of RNA. Till date a few studies are present in the literature on the interaction of KMP with different polymorphic forms of DNA and there is no published report on the binding of KMP to RNA.

EXPERIMENTAL SECTION

Materials and Methods

Materials

KMP, nucleic acids and cacodylate trihydrate (sodium salt) were purchased from Sigma Aldrich Corporation (St. Louis, MO, USA) in pure form. They were used in experimental purposes in its native state without further purification. KMP solutions were kept in dark all time to avoid any photochemical change and concentration was checked spectrophotometrically by using a known molar extinction coefficient value of 14778 M^{-1} cm^{-1} at 373 nm.[38] Molar extinction coefficient values of 9350, 7140 and 5900 $M^{-1}cm^{-1}$ at 260 nm were used to calculate the concentration of poly-U, A.U and U.A*U respectively.[46] Experimental concentration range was such that no deviation from Beer's law was observed. Fresh solutions of KMP were prepared each day for better results. 35 mM cacodylate buffer of pH 7.0 [10 mM sodium cacodylate ($Na(CH_3)AsO_2.3H_2O$), 0.1 mM Na_2EDTA and 25 mM NaCl], designated as SCH-buffer afterwards, was used to carry out all the experiments. Distilled deionized water and analytical grade reagents were used for the preparation of buffers. Buffer solutions were filtered by using millipore filters of 0.45 μm pore size.

Methods

UV-Vis Absorption experiments

All UV-Vis absorbance studies were made on a Shimadzu model UV-1800 spectrophotometer (Shimadzu Corporation, Japan) in matched quartz cells of 1 cm path length. A thermo-programmer was attached to it to maintain the temperature by peltier effect. Reverse spectrophotometric titration procedure, as described previously [47] has been exploited to probe the interaction of KMP with both U.A*U-triplex and A.U-duplex. In brief, a known concentration of U.A*U/A.U was kept in both sample and reference cells and small aliquots of a known concentration of KMP were added into the sample cell whereas equal amount of

buffer was added to the reference cell. After each addition, solution was mixed and allowed to re-equilibrate for at least 5 minutes before recording each data. Direct titration procedure was employed for single stranded poly-U. The absorbance values have been kept at the minimum for optical studies to avoid any possible aggregation.[47]

Spectrofluorimetric study.

A Shimadzu RF-5301PC spectrofluorimeter (Shimadzu Corporation, Kyoto, Japan) was used for fluorimetric titration of KMP in presence of U.A*U, A.U and singlet poly-U. A highly sensitive temperature controller was attached to this spectrofluorimeter to control the temperature of solution. Measurements were made in fluorescence free quartz cell of 1 cm path length. To a fixed concentration of KMP, increasing concentration of U.A*U, A.U and poly-U was added under constant stirring condition. After each addition, solution was allowed to equilibrate for 3 minutes. A fixed excitation and emission band pass of 5 nm were employed for all the titrations.

Evaluation of Binding Parameters.

The data obtained from Spectrophotometric and spectrofluorimetric titration were employed for constructing Scatchard plots of r/C_f versus r.[48] The binding isotherms have been found to be nonlinear and noncooperative and the plots were analyzed by excluded site model using McGhee and von Hippel equation.[49]

$$\frac{r}{C_f} = K'(1-nr)\left[\frac{(1-nr)}{\{1-(n-1)r\}}\right]^{(n-1)} \quad \ldots\ldots\ldots(1)$$

where K', n, r and C_f are the intrinsic binding constant to an isolated site, the number of the nucleotides occluded after the binding of one single ligand molecule, the number of moles of KMP bound per mole of nucleotide and free KMP concentration respectively. To determine the best-fit parameters of K' and n the plots were analyzed by using origin 7.0 software.

Determination of Binding Stoichiometry

Job's continuation method[50] was employed to determine the binding stoichiometry of KMP-RNA polymer complex. Fluorescence spectroscopy was used as a tool for finding the stoichiometry of binding. Concentration of both forms of RNA and ligand were varied but the sum of their concentrations was kept constant at 30 μM during the experiment. Corresponding fluorescence intensity change was noted at a fixed emission maxima (λ_{max}= 549 and 540 nm for RNA-triplex and duplex respectively). The relative difference in fluorescence intensity of KMP at the corresponding emission maxima was plotted against the mole fraction of KMP. The point of intersection of the plot gave the mole fraction of KMP in the bound condition. The stoichiometry was obtained in terms of RNA: KMP [$(1-\chi_{KMP})/\chi_{KMP}$] where, χ_{KMP} denotes the mole fraction of KMP. The results reported here is average of at least three experiments.

Fluorescence polarization anisotropy

Steady state fluorescence anisotropy was measured using the above mentioned spectrofluorimeter. Steady state anisotropy (r′) is defined by[51]

$$r' = \frac{(I_{VV} - G \cdot I_{VH})}{(I_{VV} + 2G.I_{VH})} \quad \ldots\ldots(2)$$

Where, G is the ratio of I_{HV}/I_{HH} used for instrumental correction. I_{VV}, I_{VH}, I_{HV} and I_{HH} represent the fluorescence signal for excitation and emission with the polarizer positions set at (0^o,0^o), (0^o,90^o), (90^o,0^o) and (90^o,90^o) respectively. The excitation wavelength was fixed at 373 nm. The excitation and emission slit widths were fixed at 5 nm. Readings were observed 5 min after each addition to ensure stable complex formation. Each reading was an average of five sets of measurement. Anisotropy values were plotted as a function of increasing U.A*U/A.U concentration.

Time resolved fluorescence anisotropy

To measure the time resolved fluorescence anisotropy, the method of Time Correlated Single-Photon counting (TCSPC) on a FluoroCube- 01-NL spectrometer (Horiba Jobin Yvon) was used. For the time resolved anisotropy the polarized fluorescence decays for the parallel [I_{VV}] and perpendicular [I_{VH}] emission polarizations with respect to the vertical excitation polarization were first collected at the emission maxima of KMP. The anisotropy decay function, r(t), was constructed from these I_{VV} and I_{VH} decays using the following equation,

$$r'(t) = \frac{(I_{VV} - G \cdot I_{VH})}{(I_{VV} + 2G.I_{VH})} \text{.....(3)}$$

The analysis of anisotropy decay was performed by using IBH DAS6 analysis software where G is the correction factor.

Fluorescence lifetime measurements

TCSPC measurements were carried out in SCH buffer at 20 °C for the fluorescence decay of KMP in absence and in presence of increasing concentration of three different forms of RNA. For the TCSPC measurements, the photo-excitation was made at 370 nm using a picosecond diode laser (IBH Nanoled 07) in an IBH fluorocube apparatus. The fluorescence decay data were collected on a Hamamatsu MCP photomultiplier (R3809) and were analyzed by using IBH DAS6 software using the following equation

$$F(t) = \sum \alpha_i e\left(\frac{t}{\tau}\right) \text{.....(4)}$$

Where, α_i is the i-th pre-exponential factor and τ is the decay time. The decay time is the life time of the excited species under consideration. The decay profiles were fitted following the χ^2 criteria. The acceptable value of χ^2 should be remained within 1.1.[52]

Mode of binding: fluorescence quenching studies

Potassium iodide was used as anionic quencher to carry out the quenching experiments. For the sake of experiment, a fixed total ionic strength was maintained by mixing KI and KCl solutions in different proportion. Fluorescence intensity changes were monitored at the emission maxima of RNA bound KMP as a function of the concentration of iodide. The data obtained from the experiment were plotted in the form of Stern-Volmer equation[53]

$$\frac{F_o}{F} = 1 + K_{SV}[Q] \text{.....(5)}$$

Where, F_o and F are the fluorescence intensities of the flavonoid complexed with RNA in absence and in presence of the quencher (Q) KI and K_{SV} is the Stern-Volmer quenching constant. Stern-Volmer quenching constant K_{SV} is indicative of the accessibility of the bulky quencher (iodide) to the fluorophore KMP. The value of K_{SV} was procured from the slope of the F_0/F *versus* [KI] plot.

Viscometric study

Viscometric measurements were carried out using a Cannon-Manning semi micro dilution viscometer type 75 (Cannon Instruments Co., State College, PA, USA) submerged vertically in a constant temperature bath maintained at 20±0.5 °C. The molecular weight of the U.A*U sample was estimated to be in the order of 2–2.4x10^5 Da with an intrinsic viscosity of 2.6 dL/g. 700 µL of 400 µM U.A*U/A.U solution was placed in the viscometer and aliquots of stock solution of KMP were directly added into the viscometer to obtain increasing D/P (KMP/nucleotide molar ratio) values. Flow times of RNA-polymers in absence and in presence of increasing concentration of KMP were measured in triplicate with an accuracy of ±0.01 s and the relative specific viscosity was calculated by using the equation:

$$\frac{\eta'_{sp}}{\eta_{sp}} = \frac{[t_{complex} - t_0]}{[t_{control} - t_0]} \text{.....(6)}$$

Where, η'_{sp} and η_{sp} are the specific viscosity of U.A*U/A.U in presence and in absence of KMP; $t_{complex}$ and $t_{control}$ are the time of flow of complex and control solution and t_o is the same for buffer solution as described previously.[9]

Thermal melting studies

The denaturation profiles of triple and double helical RNA in absence and in presence of KMP in SCH buffer were monitored in the same spectrophotometer used earlier. Corresponding changes in absorption were noted at 260 nm while scanning temperature range was from 15 °C to 70 °C.

Circular dichorism (CD) spectral studies

CD Spectra of U.A*U, A.U and poly-U in presence of KMP were recorded by JASCO J815 spectropolarimeter (Jasco International Co., JAPAN) attached with a temperature controller and a thermal programmer model PFD-425L/15 interfaced in a rectangular quartz cuvette of 1 cm path length. Each scan was accumulated at a scan speed of 100 nm min^{-1}. Sample temperature was maintained at 20 °C for each experiment. Spectra were corrected for buffer signal first and then converted to the molar elipticity ([θ]) in units of deg cm^2 $dmol^{-1}$ with the help of Jasco Standard Analysis software based on RNA-polymer concentration. Each spectrum was an average of three consecutive readings.

Temperature dependence study and evaluation of thermodynamic parameters

At four different temperatures i.e. 10, 15, 20 and 25 °C, titration of U.A*U with KMP was performed to calculate the association constant (K') at different temperatures. By employing the plot of *ln K′ versus 1/T* (van't Hoff plot) over the experimental range of study, thermodynamic parameters of the interaction were obtained. The slope of the plot determines ΔH^o (enthalpy change of the interaction).

$$\partial(lnK')/\partial(1/T) = -\Delta H°/R \quad \ldots\ldots(7)$$

The Gibbs free energy change was calculated by using the relation;

$$\Delta G^{\circ} = -RTlnK' \ldots\ldots(8)$$

The entropy change (ΔS^{o}) due to interaction was calculated by the following equation,

$$\Delta S^{o}=(\Delta H^{o}-\Delta G^{o})/T \ldots\ldots\ldots(9)$$

Thermodynamic parameters of the interaction of KMP with A.U were also estimated by employing the same procedure for appropriate comparison.

Results and Discussion

*Preparation and Characterization of U.A*U*

U.A*U triplex was prepared by following the methodology described earlier.[9] In short, initially A.U and poly-U were mixed in 1:1 molar ratio at 20 °C. The resulting solution was then heated up to 90 °C and kept at that temperature for 1 hour to ensure the complete denaturation of A.U. After that it was cooled at a rate of 1 °C/2 min up to 10 °C. After the formation of U.A*U triplex it was characterized by CD spectrum and thermal melting profile (Fig. S1). CD spectral behaviour of U.A*U, A.U and poly-U was checked before proceeding the experiment. From the spectral study it was observed that CD spectral characteristics of U.A*U was different from that of the A.U and poly-U. The appearance of a positive band below 230 nm in each spectrum of the RNA-polymers was indicative of A-form RNA structure. It is already well known that different polymorphic structures of RNA always adopt A-form structures.[9] Lowering of elipticity value of U.A*U than that of other two forms of RNA was probably because of the lowering of asymmetry of triplex. As in triplex the insertion of poly-U in the groove of duplex occurs which lowers the asymmetric nature of triplex. A biphasic cooperative transition was found from the thermal melting profile of triplex. The profile shows two melting temperatures one at 35 ºC and the other at 45 °C.[9] First transition temperature indicated the denaturation of Hoogsteen base paired third strand whereas the second transition temperature was due to denaturation of Watson-Crick base

pair. The outcome of thermal melting analysis of triplex and parent duplex was in good agreement with the published report.[9,46] Biphasic melting profile of triplex with a second transition temperature clearly confirms the stability of triplex.

UV-Vis Absorption Spectrophotometric titration

UV-Visible spectroscopic technique is the simplest technique to monitor the change due to small molecule-nucleic acid interaction. Binding of KMP with three different forms of RNA was monitored initially by UV-Vis spectrophotometry. To study the interaction between KMP and RNA polymers, UV titration of KMP was performed in SCH buffer at 20 °C by the addition of three different RNA polymers. In presence of A.U and U.A*U the spectrum of KMP was perturbed, but on addition of poly-U to a fixed concentration of KMP, the spectrum remained unchanged. During the titration two main absorption bands were appeared in UV-visible spectral range of KMP. These two types of band were assigned as band I (300-450 nm) and band II (250-258 nm) respectively.[54,55] The absorption of the cinnamoyl part (B+C) and the conjugated system of ring A and ring C of the molecule was assumed to be the main reason of such appearance of two bands. According to Z. Jurasekova the chemical change of flavonoids was due to presence of 1. 3-hydroxyl group in the C-ring 2. catechol moiety in the B-ring and 3. C-2=C-3 bond in the C-ring.[45] Although catechol moiety in B-ring was absent for KMP, still chemical change was taking place due to the presence of 3-hydroxyl group and the double bond of the C-ring. The spectral changes of KMP can be associated with the deprotonation of phenolic hydroxyl group of KMP which brings a significant bathochromic change in its UV absorption band as a result of extended conjugation. The λ_{max} of band I at 366 nm was shifted towards 376 nm upon addition of triplex to KMP (Fig. 2A). The observed hypochromic and bathochromic shift in absorption spectra of KMP bound U.A*U was due to the strong aromatic π-π stacking interaction. At pH 7.0, KMP does not possess any charge so there was no chance of electrostatic interaction

between KMP and RNA-polymers. Presence of two isosbestic points at 382 and 421 nm clearly indicate the presence of equilibrium between the free and bound KMP in solution. Titration of KMP with A.U also leads to an appreciable hypochromic change in absorption spectra consist of two isosbestic points at 385 and 412 nm respectively (Fig. 2B).

Spectrophotometric titrations were also extended to another RNA-polymer, poly-U for a comparative study. Gradual addition of poly-U to KMP leads no observable change in the UV-Visible region. This indicates absence of any interaction between KMP and poly-U in the experimental condition. To obtain the binding parameters from the titration of KMP by duplex and triplex, Scatchard plots were made in the form of r/C_f *versus* r. Non-linear, non-cooperative Scatchard plots were found (Fig. 3A and 3B) and the data points were fitted according to McGhee von-Hippel equation.[49] The binding constants for the interaction of KMP with triplex and duplex were 20 x 10^4 M^{-1} and 9.5 x 10^4 M^{-1} respectively at 20 °C. Best fit parameters values are shown in Table 1. Relatively higher binding affinity of KMP with U.A*U was attributed in terms of stronger stacking interaction and release of electrostatic expulsion between three strands of triplex upon binding. Similar type of observation was reported by Lee *et. al.* where coralyne binds strongly with T.A*T and C.G.C^+ triplex than their corresponding parent duplexes.[56] Similar behaviour has also been reported for other intercalating compounds like sanguinarine, aristololactum-β-D-glucoside.[46,57] Our laboratory recently reported stronger binding of chelerythrine, a naturally occurring alkaloid with triple stranded RNA compared to double stranded RNA.[9] Here, in the present study KMP showed preferential binding interaction with U.A*U triplex than A.U duplex.

Fluorescence Spectroscopy

Fluorescence spectroscopic titration is very much useful and sensitive technique to study the interaction of small molecule and nucleic acid. It is of more advantageous over other tools because of its high sensitivity, large linear concentration range. In our experimental

condition, titration of KMP with RNA-triplex (Fig. 4A) and duplex (Fig. 4B) causes a marked increase in fluorescence intensity whereas no change was observed for single stranded poly-U. Enhancement of emission intensity basically supports the interaction of triple and double helical RNA with KMP. Enhancement of emission intensity was much more in case of triplex-KMP than duplex-KMP complex. But in both cases KMP showed dual fluorescence behavior. Two emission maxima were seen rather than one maximum due to the presence of hydroxyl group in both 3 and 5 position of KMP molecule. Kasha and his group already reported that 3-hydroxyflavone and 5-hydroxyflavone exhibited dual fluorescence behavior.[58] Pradhan *et. al* recently reported that at pH 7.0 KMP showed dual fluorescence behaviour on interaction with DNA.[39] In our experimental condition the appearance of two peaks, one at around 538 nm was for photoproduced isomer whereas the other at 432 nm was for normal tautomeric species. This observation was accounted as two tautomeric species were present in both cases. But in case of triplex-KMP complex the extent of increment of fluorescence intensity of 538 nm peak was more than duplex-KMP complex. Enhancement of emission intensity of the tautomeric species indicated that addition of triplex to KMP favours excited state intramolecular proton transfer process (ESIPT).[42] The data were then cast in the form of Scatchard plot for evaluation of binding parameters.[48] Calculated binding constant and the stoichiometry of binding are presented in Table 1. Nearly same value of binding constant was obtained from the fluorimetric titration when compared with the spectrophotometric data. Comparatively higher binding constant for U.A*U-KMP complex was seen than A.U-KMP complex.

Stoichiometry of Binding: Job's plot

Binding stoichiometry of the interaction was again evaluated with the help of Job's plot by using fluorescence data. Single binding mode of KMP with double and triple helical forms of RNA was revealed from the plot (Fig. 5) of relative fluorescence intensity *versus* mole

fraction of KMP. The intersection point was at χ_{KMP}=0.21 for KMP-triplex and χ_{KMP}=0.26 was for KMP-duplex complex. Binding stoichiometry calculated from the data was ~3.85 and ~2.81 respectively for triplex and duplex bound KMP. The result obtained is in good accordance with the data obtained from spectrophotometric and spectrofluorimetric titration.

Steady State Fluorescence Polarization Anisotropy

Fluorescence polarization anisotropy is a tool that helps us to know the nature of the surroundings of biological probes. The anisotropy value is influenced by a molecule's shape, size and flexibility.[53] Anisotropy value provides the information about the probable location of probe in micro-heterogeneous environment of nucleic acids. The more the rigidity of the surroundings of probe, the more will be anisotropy value. The change of anisotropy value with increasing concentration of RNA-polymer is presented in Fig. S2. It was found that anisotropy value was increased three fold upon binding from the initial value in case of RNA-U.A*U complex whereas two fold increment in the anisotropy value was obtained in case of A.U under identical condition. This result corroborates the fact that on binding with RNA triplex KMP was trapped in a more motionally restricted region than duplex RNA. Intercalation of KMP in between the bases of RNA triplex may be the probable cause of such behavior.

Time Resolved Fluorescence Anisotropy

To get a vivid idea about the microenvironment of the bound KMP in the helix the time resolved anisotropy decay measurements were performed. It is a sensitive tool for ascertaining the information about the rotational relaxation of the bound probe. Fig. 6 represents the corresponding anisotropy decay of free and bound KMP. The anisotropy decay of KMP is mono exponential in nature initially. Whereas the decay profiles of bound KMP showed remarkable dip and rise profiles dictating two correlation times. Such results affirm the presence of two components in the excited state, one with a reasonably shorter lifetime

than another. The two lifetime values differ in ten times than other can be interpreted as faster motion, i.e. smaller lifetime value was for the exposed KMP molecule in solvents and the slower motion was for the bound counterpart of the fluorophore. This type of decay behavior has been described by Lakowicz earlier.[53] The dip and rise pattern of the bound KMP in the duplex and triplex environment originated from the presence of free and bound KMP. The dip was more in case of triplex bound KMP mostly signify that the KMP is bound with triple helical forms more strongly than double helical forms of RNA.[53]

Fluorescence Lifetime Study

Lifetime study serves as an indicator of the local surroundings of fluorophore and its response towards excited state interaction. The time resolved fluorescence decay of KMP by following TCSPC technique was recorded in absence and in presence of U.A*U and A.U. Representative fluorescence decay profiles of KMP in free and bound condition is presented in Fig. 7. The appearance of biexponential decay profile of free KMP molecule was probably due to the presence of two isomers of KMP i.e. normal and photoproduced isomer. The lifetime value of the first component was remaining almost same on addition of both forms of RNA. But the lifetime value of second component was changed from 4.7 ns to 8.4 and 7.9 ns at saturation for U.A*U and A.U bound KMP respectively. The shorter lifetime value was probably for the unbound KMP. The increase in shorter lifetime, though a little bit, with increasing concentration of RNA may be the presence of ordered solvent environment around the helix of RNA.[55] Increase in lifetime value on binding was basically for the stronger binding of KMP with both forms of RNA.

Fluorescence Quenching Experiments

Fluorescence quenching experiments supply additional information based on the location of small molecule. The mode of interaction was ascertained from the quenching study. Molecules that are free or bound on the surface are easily available to the quencher, while

that are intercalated in between base pairs are not. We have used iodide as the quencher here. In presence of it fluorescence intensity of free KMP is decreased. But on addition of quencher to the U.A*U bound KMP, the emission intensity remained almost same. This result can be interpreted on the basis of the fact that KMP was inserted in between the base doublet or triplet of RNA. So, in presence of quencher, KMP cannot come in close contact with iodide. Iodide, being negatively charged cannot make a way into the core of RNA helix without avoiding the repulsion of negatively charged phosphate groups around the helix. It is already a well established phenomenon that in case of intercalation, quenching constant should be less compared to free small molecules.[58] In presence of iodide, emission intensity of A.U bound KMP was also decreased but in a lesser extent. Stern Volmer quenching constants (K_{SV}) were found to be 4.0, 3.24 and 1.4 M^{-1} for free, A.U bound KMP and U.A*U bound KMP respectively as obtained from Fig. 8. Reduction in K_{SV} values on interaction with U.A*U was actually for the less accessibility of KMP towards quencher. Corresponding results were suggestive for intercalation. Less decrease in K_{SV} value in case of A.U was probably for partial intercalation of KMP in to the base pairs of A.U.

Viscosity Measurement

Viscosity measurement is a hydrodynamic method for evaluating the binding mode of interaction of KMP with different forms of RNA. Viscosity measurement is a very convenient tool for evaluation of binding mode of small molecules to nucleic acid. Viscosity value is highly sensitive to change in length of RNA-polymers. Fig. 9 represents the viscosity data of KMP bound U.A*U and A.U in solution. The relative specific viscosity value is increased with increase in D/P ([KMP]/[U.A*U/ A.U]) ratio. This value was almost constant for poly-U in free and bound condition. The change was more in case of KMP bound triple helical forms of RNA. Lerman[59] proposed that in intercalation mode of binding small molecules inserted in between bases of nucleic acids which causes elongation of helix chain

length and as well as increase in viscosity of solution. Our results clearly decipher that KMP binds with U.A*U by intercalation mode of binding. In this mode of binding base pairs of RNA stiffens and lengthen in order to accommodate the KMP in between the base pairs. Though relative increase in viscosity of A.U on addition of KMP was lower compared U.A*U, still there was a marked increase in the viscosity value. The mode of binding of A.U with KMP was not true intercalation. Both quenching and viscosity data suggest together that the mode of binding of KMP was intercalation in case of U.A*U whereas it was partial intercalation for A.U.

Thermal Melting Study

Thermal denaturation studies focus on the stabilization of nucleic acid on binding with small molecules. Increasing the temperature of solution of double or triple helices generates single stranded nucleic acid. The temperature that marks the midpoint of the melting profiles is called melting temperature (T_m). At this temperature half of the nucleic acid exists in helical form and other half exists in single stranded form. To study the interaction as well as the stabilization effect of KMP on Hoogsteen third strand and Watson-Crick double strand, thermal melting study was carried out in absence and in presence of KMP by noting the change in absorbance value at 260 nm. Thermal melting temperatures (T_m) of free U.A*U were at 34 and 45 °C respectively. First melting temperature denotes the denaturation of Hoogsteen base paired third strand whereas second transition was for the denaturation of Watson-Crick base pair. On binding with KMP third strand was stabilized nearly 14 °C and Watson-Crick double strand was stabilized up to 3 °C (Fig. 10 A & 10 B). Thermal melting temperature of free A.U was at 44 ^{o}C. KMP shows comparatively small effect on thermal melting temperature of A.U but exhibit a remarkable change on the stabilization of Hoogsteen base pair third strand of U.A*U triplex. It is already an established phenomenon that intercalation and stacking interaction of small molecules with DNA or RNA increases

melting temperature of nucleic acid.[60] Experimental outcome of thermal melting study was an indicative of intercalation mode of binding of KMP with U.A*U and partial intercalation mode of binding with A.U. The melting profiles of our experiment are shown in Fig. 10 and the data are summarized in Table 2. A recent report by Pradhan *et. al.* showed that protonated DNA was stabilized upon binding with KMP, quercetin and morin.[38,39] Stabilization of Watson-Crick base pair second strand instead of Hoogsteen base pair third strand of U.A*U by phenosafranin has been narrated by the same author.[61] Chelerythrine, a benzophenanthridine intercalator has also been reported to stabilize the third strand of RNA-triplex as well as the Watson-Crick base pair of the triple helical nucleic acid.[9] Basically intercalators possess flat heteroatomic aromatic ring system that can intercalate in between the base pairs of triple helical forms of RNA whereas groove binders are typically composed of various aromatic rings i.e. pyrrole, furan or benzene that are connected via torsion free bonds. The complex formed by intercalation mode of binding is generally stabilized by π- π interaction between the drug and RNA-polymer molecule. In general, intercalation increases the melting temperature of RNA-triplex and duplex. Intercalation also results in perturbation in the chain length of RNA-polymer which is reflected in the viscometric result. Along with intercalation mode of binding, there also exists another hydrophobic interaction, groove binding interaction. Different classes of compound like pluramycin, alfatoxin, aminoglycoside belongs to major groove binding natural products.[62] Torsional freedom along the joining bonds of groove binders enables them to twist and became isohelical with the groove of nucleic acids. Neomycin, an aminoglycoside acts as a groove binder towards nucleic acids. Presence of non aromatic moiety in this compound leads to its limitation to behave as groove binding agent. It has been already reported that it stabilized only the third strand of triplex without causing any remarkable effect on the denaturation of duplex.[11]

Circular Dichorism study

CD spectroscopy is a useful technique in evaluating the changes in RNA-morphology during RNA-flavonoid interaction. Non-covalent RNA-drug interactions affect the structure of RNA, which causes perturbation in the intrinsic spectra of RNA in UV-Visible range. It is already a well known fact that in electrostatic or groove binding of small molecules with nucleic acid causes very less perturbation in base stacking and helicity while in case of intercalation significant changes were observed.[63] In our experimental condition titration of RNA-triplex with KMP (Fig. 11 A) leads observable changes in CD spectral behavior whereas minor changes was seen when A.U was titrated with KMP (Fig. 11 B). CD spectral behavior of triple helical nucleic acid on binding with KMP supports intercalation. But less perturbation in CD spectra of A.U in presence of KMP supports in favour of partial intercalation of KMP inside the double helix. Presence of an isoelliptic point at 258 nm in CD spectra of U.A*U by KMP gives information about the presence of equilibrium between bound and free nucleic acid. Positive band at 260 nm of U.A*U shifts towards 265 nm on binding with KMP.

Evaluation of thermodynamic parameters of the interaction

Understanding the thermodynamics of small molecules binding to RNA polymer is of both practical and fundamental interest. Thermodynamic studies offer the key insight in to the molecular forces that drive complex formation on binding. It cannot be obtained from computational study that is why we have measured it experimentally by calculating different association constants at different temperatures at the constant salt molarity of 35 mM [Na^+]. The binding constant values were decreased simultaneously with increase in temperature for both RNA-polymers. By using these data van't Hoff plots of lnK' *versus 1/T* were plotted (Fig. 12). The linear plot dictates the negligible heat capacity change of the interaction in the specified range of temperature used here. Calculated binding parameters are presented in

Table. 3. Corresponding data for the interaction of KMP with U.A*U and A.U revealed that the association was favored by negative enthalpy and positive entropy change. Negative enthalpy change might be arising from the contribution of van der Waals interaction as well as from hydrophobic or electrostatic interaction. Binding free energy change mainly resulted from the contributions from conformational changes in RNA and flavonoids upon complex formation, hydrophobic transfer of KMP from bulk solution into its binding site. The removal of non polar drug molecule from aqueous environment is entropically favourable due to the disruption of hydration layer around the KMP molecules upon intercalation. Localized unwinding of triplex on binding with KMP by intercalation mode of fashion causes an increase in the distance between adjacent phosphates on the backbone. Both of these effects are responsible for causing positive entropy change during the interaction. In intercalation binding, an additional van der Waals interaction was involved in between the KMP and adjacent base pairs of RNA-polymers that are also capable of providing a significant contribution to the negative free energy change.

Conclusion

The outcome of our study about the interaction of KMP with triple, double and single helical forms of RNA are presented here with the relevant experimental findings. The study highlighted on the fact that KMP exhibits comparatively higher binding constant with U.A*U other than A.U in the specified experimental condition. No interaction was seen with poly-U in the experimental condition. Hypochromic and bathochromic shift in UV-absorption spectra of KMP on titration with U.A*U/A.U initially manifest intercalation as the mode of binding. Moreover reduction in Stern Volmer constant of U.A*U-KMP complex compared to free KMP also demands the mode of binding of KMP to U.A*U as intercalation. The results of viscometric measurements and thermal melting study together confirm the binding of KMP with U.A*U as intercalation. Whereas the binding mode of KMP with A.U was not true

intercalation rather it was partially intercalated in between the base pairs. A little change in thermal melting temperature of A.U–KMP complex compared to A.U, less perturbation in CD spectra of A.U by KMP as well as absence of bathochromic shift in the absorption spectra of KMP upon binding confirmed the mode of binding as partial intercalation. Third strand of triplex was stabilized about 14 ^{o}C by KMP, whereas Watson-Crick base paired second strand was stabilized only 3 ^{o}C. Thermodynamic data of the interaction of KMP with triplex provides the information about the nature of interaction as well as focus on the driving force of the interaction. The free energy change of binding was mainly due to the exothermic nature of drug-RNA-triplex/duplex binding. Linear van't Hoff plot of the binding of KMP with both forms of RNA implies that heat capacity change was negligible. Positive entropy changes might arise due to release of water molecules from the hydration shell of RNA, release of counter ions and for stronger binding interaction. The binding constant data revealed that binding interaction of KMP was stronger for triplex than its corresponding parent duplex. Since the interaction of naturally occurring small molecules with RNA-polymer is a promising field in research of medicinal science, this study brings out the scope of exploring the flavonoids as antiviral drugs.

Acknowledgement

S.D. gratefully acknowledges the financial assistance provided by the University Grant Commission (UGC), New Delhi, India [F. No. 43-243/2014 (SR), MRP-MAJORCHEM-2013-37991]. LH and ABP thank to the UGC, Government of India for the award of senior research fellowship. SB thanks the University Grant Commission, Government of India, for the award of RGNF Research Fellowship. Richa Tiwari thanks to University Grant Commission (UGC), New Delhi, India [F. No. 43-243/2014 (SR), MRP-MAJORCHEM-2013-37991] for Project Fellowship.

References

1. J. D. Watson and F. H. C. Crick, *Nature*, 1953,**171**, 737-738.
2. G. Felsenfeld and A. Rich, *Biochim. Biophys. Acta*, 1957, **26**, 457–468.
3. G. Felsenfeld, D. R. Davies and A. Rich, *J. Am. Chem. Soc.,* 1957, **79**, 2023–2024.
4. E. Tuite and B. Norden, *Bioorg. Med. Chem.*, 1995, **3**, 701-711.
5. S. Basili, A. Bergen, F. Dall'Acqua, A. Faccio, A. Granzhan, H. Ihmels, S. Moro and G. Viola, *Biochemistry,* 2007**, 46***,* 12721-12736.
6. M. Keppler, O. Zegrocka, L. Strekowski and K. R. Fox, *FEBS Lett.*, 1999, **447**, 223-226.
7. A. Arora, N. Kumar, T. Agarwal and S. Maiti, *FEBS J.*, 2010, **277**, 1345.
8. H. Sun, J. Xiang, Y. Tang and G. Xu, *Biochem. Biophys. Res. Comm.*, 2007, **352**, 942–946.
9. L. Haque, A. B. Pradhan, S. Bhuiya and S. Das, *Phys. Chem. Chem. Phys*., 2015, **17**, 17202-17213.
10. T. Biver, N. Busto, B. Garcia, Jose M. Leal, L. Menichetti , F. Secco and M. Venturini, *J. Inorg. Biochem.,* 2015, **151**, 115-122.
11. D. P. Arya, R. L. Coffee, J. B. Willis and A. I. Abramovitch, *J. Am. Chem. Soc*, 2001, **123,** 5385-5395.
12. D. P. Arya, L. Micovic, I. Charles, R. L. Coffee, J. B. Willis and L. Xue, *J. Am. Chem. Soc*, 2003, **125**, 3733-3744.
13. D. P. Arya, R. L. Coffee and I. Charles. *J. Am. Chem. Soc*. 2001, **123**, 11093-11094.
14. H. J. Lozano, B. García, N. Busto and J. M. Leal, *J. Phys. Chem. B*, 2013, **117**, 38−48.
15. S. E. Butcher and A. M. Pyle*, Acc. Chem. Res.*, 2011, **44**, 1302–1311.
16. F. A. Buske, J. S. Mattick and T. L. Bailey, *RNA Biol.,* 2011, **8**, 427–439.
17. N. K. Conrad, *WIREs RNA,* 2014, **5**, 15–29.
18. D. P. Arya, *Acc Chem. Res.,* 2011, **44,** 134-146

19. D. P. Arya, L. Xue and B. Willis, *J. Am. Chem. Soc.,*2003, **125,** 10148-10149.

20. R. Silvers, H. Keller, H. Schwalbe and M. Hengesbach, *Chem.BioChem.*, 2015, **16**, 1109-1114.

21. J. Y. Chin, E. B. Schleifman and P.M. Glazer, *Front Biosci.,* 2007, **12**, 4288-97.

22. E. B. Schleifman J. Y. Chin and P.M. Glazer, *Methods Mol Biol.,* 2008, **435,** 175-90.

23. G. Devi, Y. Zhou, Z. Zhong, D. K. Toh and G. Chen, *Wires RNA*, 2015, **6**, 11-128.

24. X. J. He and L. F. Tan, *Inorg. Chem*., 2014, **53**, 11152-11159.

25. R. Sinha and G. S. Kumar, *Biophys. Chem*., 2009, **113**, 13410-13420.

26. G. Rusak, I. Piantanida, L. Masi , K. Kapuralin, K. Durgo and N. Kopjar, *Chem. Biol. Interact.*, 2010, **188**, 181–189.

27. C. A. Rice Evans, N. J. Miller and G. Paganga, *Free Radic. Biol. Med*., 1996, **20**, 933–956.

28. E. Brown, H. Khodr, R. C. Hider and C. A. Rice-Evans, *Biochem. J.*, 1998, **330**, 1173–1178.

29. G. Deng, X. W. Fang and J. L. Wu, *Radiat. Phys. Chem*., 1997, **50**, 271–276.

30. M. Kawai, T. Hirano, S. Higa, J. Arimitsu, M. Maruta, Y. Kuwahara, T. Ohkawara, K. Hagihara, T. Yamadori, Y. Shima, A. Ogata, I. Kawase and T. Tanaka, *Allergol. Int*., 2007, **56**, 113–123

31. A. Garcia-Lafuente, E. Guillamon, A. Villares, M. A. Rostagno and J. A. Martinez, *Inflamm. Res.*, 2009, **58**, 537–552.

32. T. P. T. Cushnie and A. J. Lamb, *Int. J. Antimicrob. Agents*, 2011, **38**, 99–107

33. M. K. Chahar, N. Sharma, M. P. Dobhal and Y. C. Joshi, *Pharmacogn. Rev.*, 2011, **5**, 1–12

34. C. Wan, M. Cui, F. Song, Z. Liu and S. Liu*, Int. J. of Mass Spectrometry, 2009,* **283**, 48–55

35. W. Li, M. Zhang, J. L. Zhang, H.Q. Li, X.C. Zhang, Q. Sun and C. M. Qiu, *FEBS Lett*., 2006, **580**, 4905-4910.

36. H. Sun, Y. Tang, J. Xiang, G. Xu, Y. Zhang, H. Zhang and L. Xu, *Bioorg. Med. Chem. Lett.* 2006, **16**, 3586-3589.

37. H. Sun, J. Xiang, Y. Tang and G. Xu, *Biochem. Biophys. Res. Co*., 2007, **352**, 942-946.

38. A. B. Pradhan, L. Haque, S. Bhuiya and S. Das, *RSC Adv.*, 2015, **5**, 10219-10230.

39. A. B. Pradhan, L. Haque, S. Bhuiya, A. Ganguly and S. Das, *J. Phys. Chem. B.,* 2015, **119**, 6916−6929.

40. C. D. Kanakis, P. A. Tarantilis, M. G. Polissiou and H. A. Tajmir-Riahi*, DNA and Cell Biol.*, 2006, **25,** 116-123.

41. M. Marini, I. Piantanida, G. Rusak and M. Zini, *J. Inorg. Biochem*., 2006, **100**, 288–298.

42. M. Tungjai, W. Poompimon, C. Loetchutinat, S. Kothan, N. Dechsupa and S. Mankhetkorn, *The Open Drug Delivery Journal,* 2008, **2,** 10-19.

43. A. Y. Che and Y. C. Chen, *Food Chemistry*, 2013, **138**, 2099–2107.

44. C. D. Kanakis, S. Nafisi, M. Rajabi, A. Shadaloi, P. A. Tarantilis , M. G. Polissiou , J. Bariyanga and H. A. Tajmir-Riahi, *Spectroscopy*, 2009, **23,** 29–43.

45. Z. Jurasekova, C. Domingo, J. V. Garcia-Ramosb and S. Sanchez Cortes, *Phys. Chem. Chem. Phys.*, 2014, **16**, 12802–12811.

46. A. Ray, G. S. Kumar, S Das and M. Maiti, *Biochemistry,* 1999**, 38***,* 6239-6247.

47. S. Das, G. S. Kumar and M. Maiti*, Biophys. Chem.*, 1999, **76**, 199-218.

48. G. Scatchard, *Ann N. Y. Acad Sci.,* 1949, **21,** 660-762.

49. J. D. McGhee and v. Hippel, *J. Mol. Biol.,* 1974, **86,** 469-489.

50. P. Job, *Annali di Chimica Applicata,* 1928, **9**, 113-203.

51. A. B. Pradhan, L. Haque, S. Roy and S. Das, *Plos ONE*, 2014, **9**, e87992.

52. L. Haque, A. B. Pradhan, S. Bhuiya and S. Das, *J. of Lumin.,* 2016, **173**, 44–51.

53. J. R. Lakowicz, Principles of Fluorescence Spectroscopy; *Plenum Press: New York, U.S.A.*, 2006.

54. F. Zsila, Z. Bikadi and M. Simonyi, *Biochem. Pharmacol*., 2003, **65**, 447–456.

55. L. Huang and D. Q. Yu, *The Application of Ultra-violet Spectroscopy in Organic Chemistry, Scientific Press*, Beijing, 1988.

56. J. S. Lee, L. J. P. Latimer and K. J. Hampel, *Biochemistry* 1993, **32,** 5591-5597.

57. M. Maiti, S. Das, A. Sen, A. Das, G. S. Kumar and R. Nandi, *J. of Biomol. Struct. & Dyn.*, 2002, **20,** 1-8.

58. E. Falkovskaia, P. K. Sengupta and M. Kasha, *Chem. Phys. Letters*, 1998, **297**, 109–114.

59. L. S. Lerman, *J. Mol. Biol.,* 1961, **3,** 18-30.

60. C. Sengupta and S. Basu, *RSC Adv***,** 2015, **5**, 78160-78171.

61. A. B. Pradhan, H. K. Mondal, L. Haque, S. Bhuiya and S. Das, *Int. J. of Biol. Macromol.*, 2016, **86**, 345–351.

62. P. L. Hamilton and D. P. Arya, *Nat. Prod. Rep*, 2012, **29**,134-143.

63. S. U. Rehman, T. Sarwar, M. A. Husain, H. M. Ishqi and M. Tabish, *Arch. Biochem. Biophys.*, 2015, **576**, 49–60.

Table 1

Binding parameters for the interaction of KMP with U.A*U and A.U in SCH buffer at 20 °C obtained from spectrophotometry and spectrofluorimetry.[a]

Parameters	Methods	Triplex	Duplex
K' x10^{-4}, the intrinsic binding constant (M^{-1})	[A] Spectrophotometry	20.0±2	9.5±0.5
	[B] Spectrofluorimetry	19.0±1	10.0±0.3
n, the no of base excluded	[A] Spectrophotometry	3.90±0.15	2.22±0.14
	[B] Spectrofluorimetry	3.70±0.14	2.50±0.10
K_{SV}, the Stern Volmer quenching constant (L mol^{-1})	Spectrofluorimetry	Free: 4.0±0.10 Bound: 1.40±0.20	Free: 4.00±0.20 Bound: 3.2±0.20
Stoichiometry from Job's plot	Spectrofluorimetry	3.85±0.15	2.81±0.10

[a] Average of three determinations

Table 2

Effect of KMP on the thermal stability of U.A*U and A.U.

RNA/Complex	D/P	T_m(°C) 3→2	T_m(°C) 2→1	ΔT_m(°C) 3→2	ΔT_m(°C) 2→1
U.A*U	0	35	46		
U.A*U+KMP	0.5	38	47.5	2.0	1.5
	1.0	49	49.0	14	3.0
A.U	0		45.0		
A.U+KMP	1.0		48.0		3.0

Table 3

Thermodynamic parameters for the interaction of KMP with U.A*U and A.U from temperature dependence spectrophotometric study.

	Temperature (K)	K'x10^{-5} M^{-1}	$\Delta G°_{293K}$ (kcal.mol^{-1})	$\Delta H°$ (kcal. mol^{-1})	$T\Delta S°$ (kcal.mol^{-1})
U.A*U	283	14.0±0.5	-7.14±0.40	-6.10±0.20	1.04±0.10
	288	6.8±0.3			
	293	2.0±0.2			
	298	1.4±0.1			

	Temperature (K)	K'x10^{-4} M^{-1}	$\Delta G°_{293K}$ (kcal.mol^{-1})	$\Delta H°$ (kcal. mol^{-1})	$T\Delta S°$ (kcal.mol^{-1})
A.U	288	9.9±0.4	-6.70±0.3	-5.30±0.22	1.40±0.12
	293	9.5±0.5			
	298	3.9±0.1			
	303	3.3±0.2			

Figure legend

Fig. 1. Chemical structure of KMP.

Fig. 2. A. UV spectra of KMP (5.2 µM, Curve 1) and bound KMP in presence of saturating concentrations of U.A*U (Curve 2) in SCH buffer at 20 °C. **B**. UV spectra of KMP (5.2 µM, Curve 1) and bound KMP in presence of saturating concentrations of A.U (Curve 2) in SCH buffer at 20 °C.

Fig. 3. Scatchard plot for the binding of KMP with U.A*U triplex (panel A) and A.U duplex (panel B). The solid lines are the non linear least squares best fit of the experimental points to the Von-Hippel equation.

Fig. 4. Representative fluorescence emission spectral changes of KMP in presence of U.A*U and A.U in SCH buffer at 20 °C. (A) curves 1-8 denote the emission spectrum of CHL (3.0 µM) treated with 0, 2.5, 5.0, 7.5., 10.0, 12.5, 15.0 and 20.0 µM of triplex respectively. (B) curves 1-6 denote the emission spectrum of CHL (3.0 µM) treated with 0, 2.05, 4.10, 6.15, 10.25 and 16.4 µM of duplex respectively. The excitation wavelength was 373 nm at a spectral excitation and emission bandwidth of 5 and 5 nm, respectively.

Fig. 5. Continuous variation plot for the binding of KMP with U.A*U triplex (panel A) and A.U duplex (panel B) in SCH buffer at 20 °C. The relative difference in fluorescence intensity at 549 and 540 nm was plotted respectively against the mole fraction of KMP added.

Fig. 6. Representative time-resolved fluorescence anisotropy decay profile of KMP in free (panel A) and bound state (panel B, -●- for A.U and -●- for U.A*U) in SCH buffer at 20 °C.

Fig. 7. Time resolved fluorescence decay curves (logarithm of normalized intensity *versus* time in nanosecond) for KMP in absence and in presence of increasing concentration of U.A*U (A) and (B) A.U at 20 °C in SCH buffer , A: profiles for free (3.0 µM) KMP (-●-) treated with 2.1 µM (-●-), 4.2 µM (-●-) and 5.3 µM (-●-) U.A*U .B: profiles for free (3.0 µM) KMP (-●-) treated with 2.1 µM (-●-) 4.2 µM (-●-) and 5.0 µM (-●-) A.U.

Fig. 8. Stern-Volmer plots for the quenching of KMP fluorescence by KI in the absence (●) and in presence of U.A*U triplex (●) and A.U duplex (●) in SCH buffer at 20 °C.

Fig. 9. A plot of change of relative specific viscosity of U.A*U triplex (●) and A.U duplex (●) with increasing concentration of KMP in SCH buffer at 20 °C. The concentrations of triplex and duplex were 500 μM.

Fig.10. Thermal melting profiles of U.A*U triplex (panel A) and A.U duplex (panel B) in absence and in presence of CHL. (A) 20.0 μM U.A*U triplex (-●-) and its complexation CHL at D/P of 0.5 (-●-), 1.0 (-●-) (B) 20.0 μM A.U duplex (-●-) and its complexation CHL at D/P of 1.0 (-●-) in SCH buffer.

Fig. 11. (A) Circular dichroic spectra of U.A*U triplex (25.0 μM) treated with varying concentrations of KMP in SCH buffer at 20 °C. (A) Curves 1-7 represent the CHL concentrations of 0, 1.6, 3.2, 4.9, 6.4, 7.8 and 10.5 μM respectively. (B) Circular dichroic spectra of duplex (25.0 μM) with varying concentrations of CHL in SCH buffer at 20 °C. The curves 1–4 represent the CHL concentrations of 0, 1.7, 4.9 and 9.6 μM respectively.

Fig.12. van't Hoff plot for complexatation of KMP with U.A*U (panel A) and A.U (panel B) in SCH buffer at different temperatures.

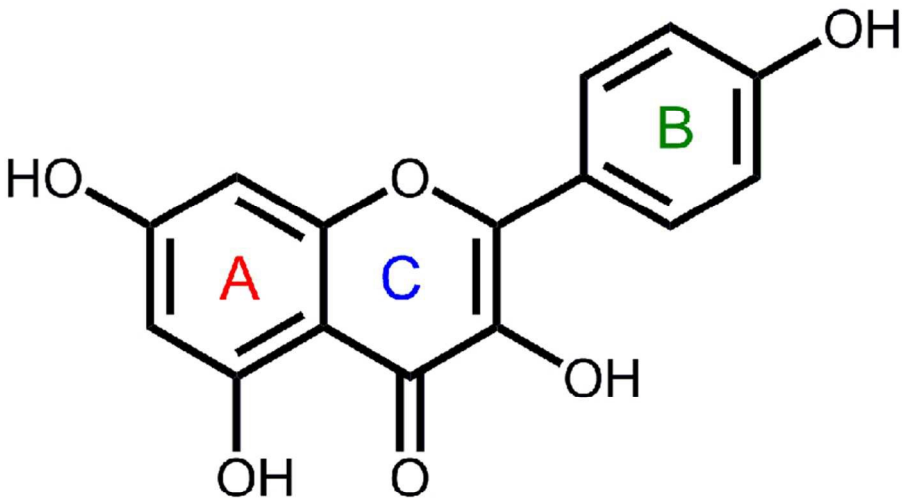

Fig. 1

76x50mm (300 x 300 DPI)

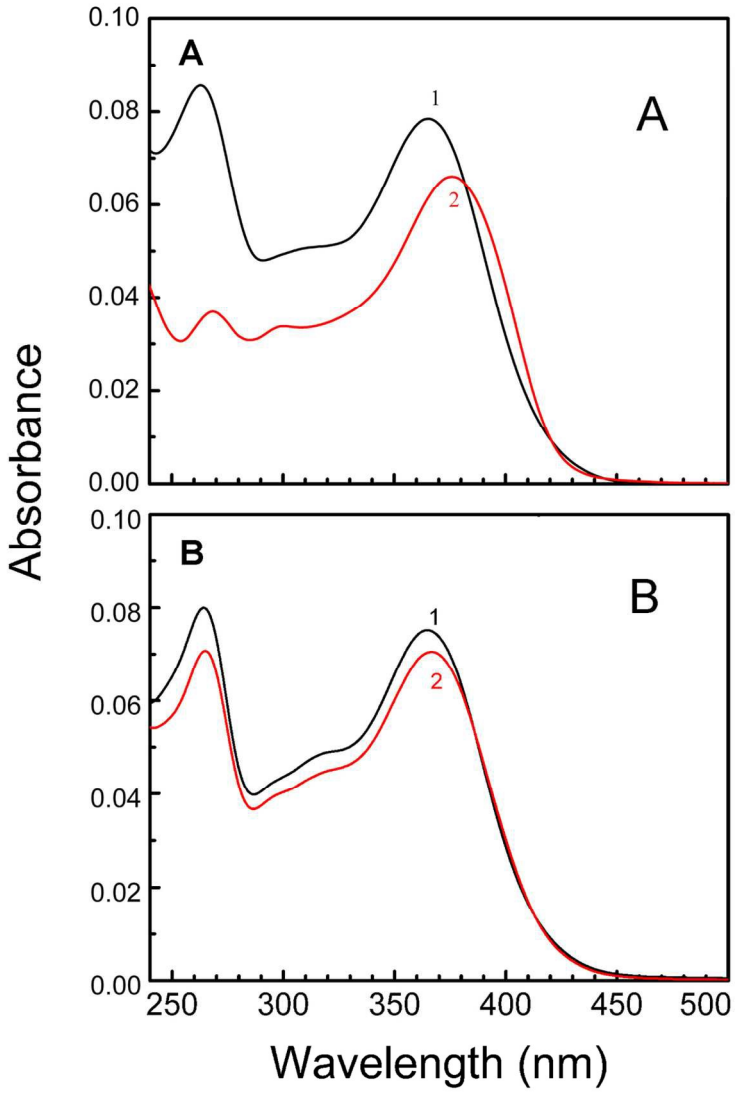

Fig. 2

107x156mm (300 x 300 DPI)

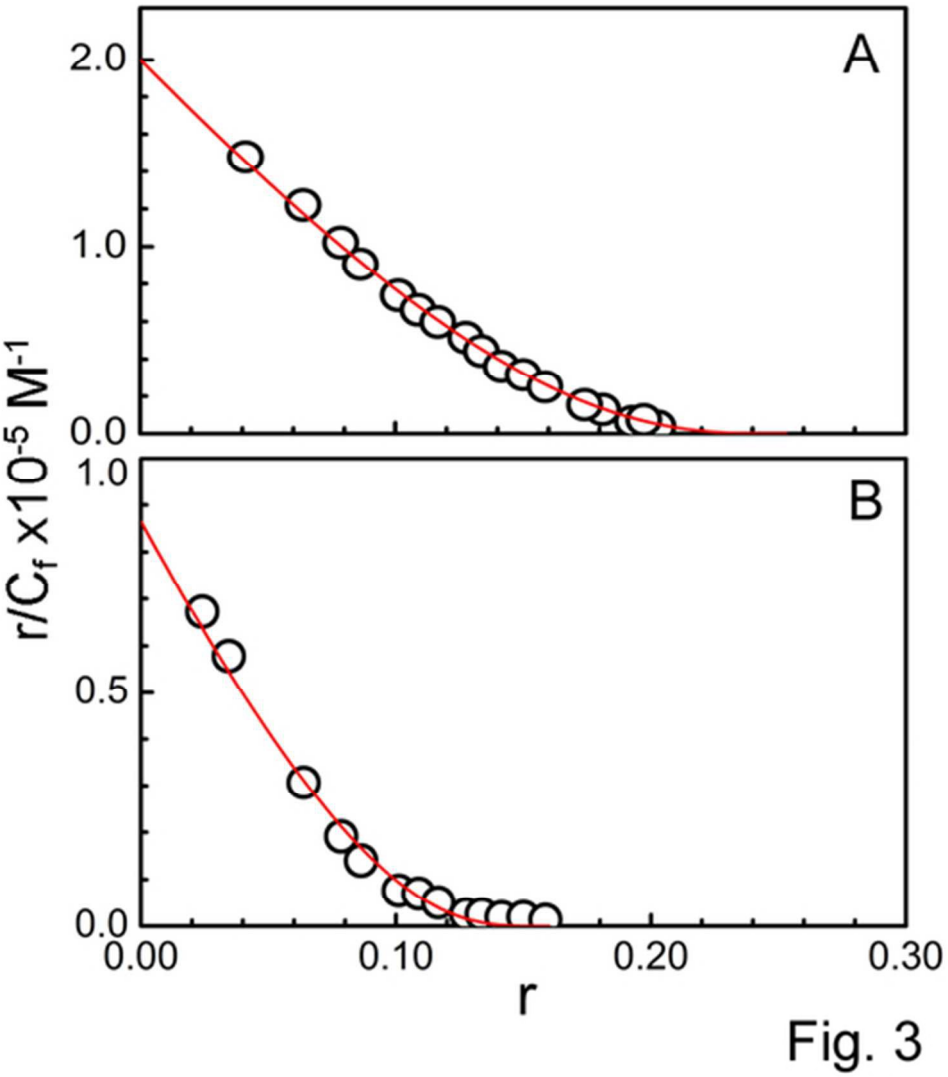

Fig. 3

44x50mm (300 x 300 DPI)

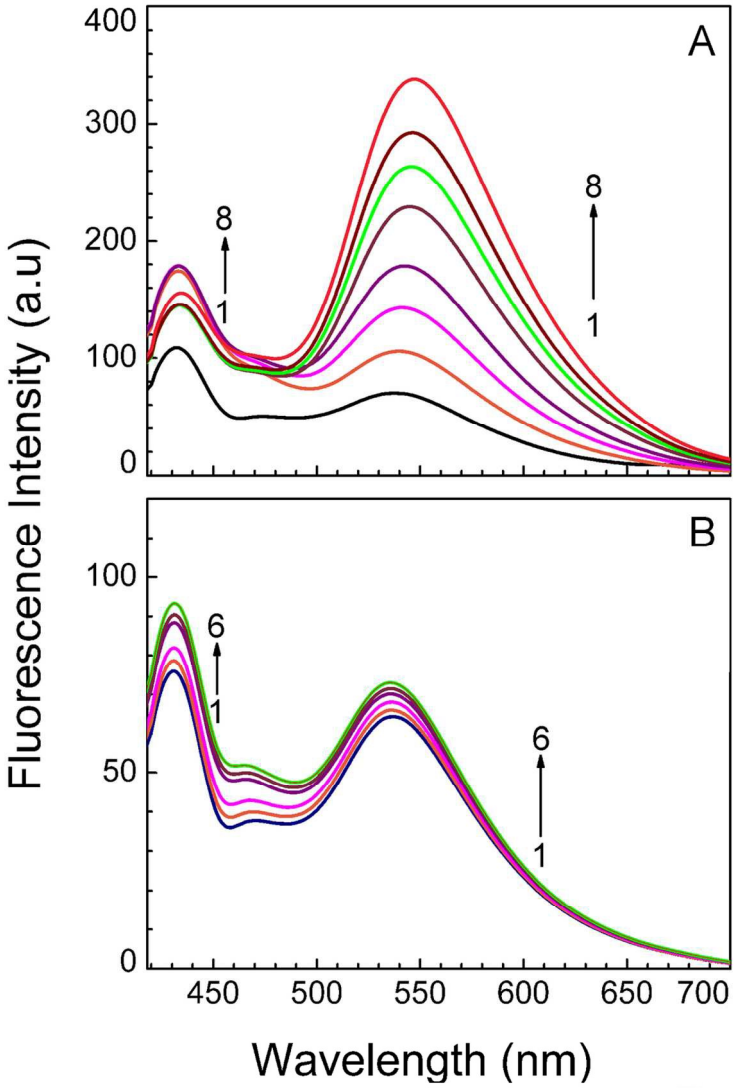

Fig. 4

107x152mm (300 x 300 DPI)

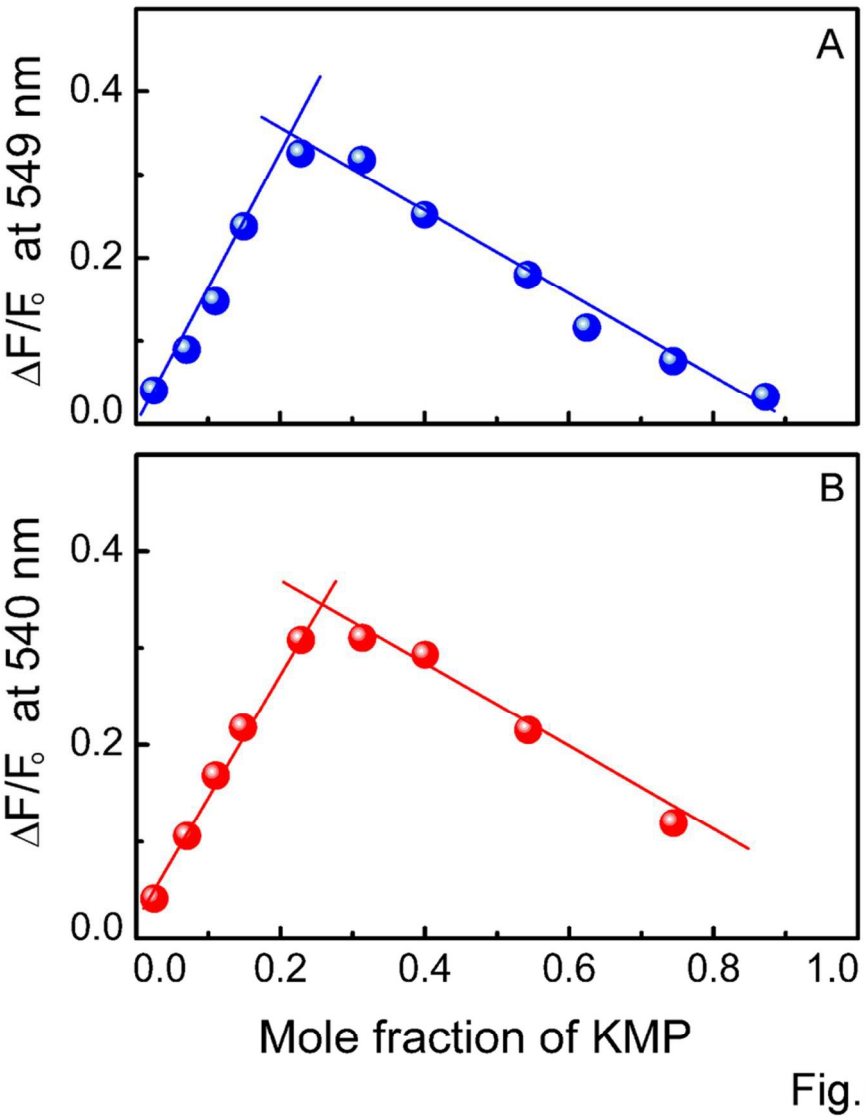

Fig.5

84x99mm (300 x 300 DPI)

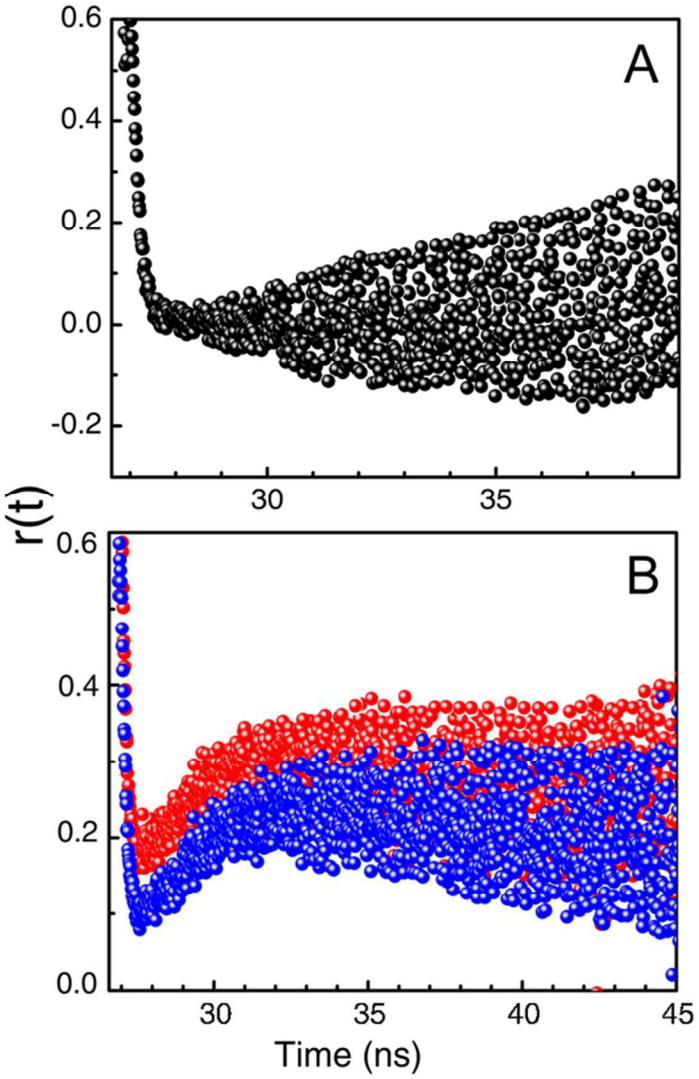

Fig. 6

56x88mm (300 x 300 DPI)

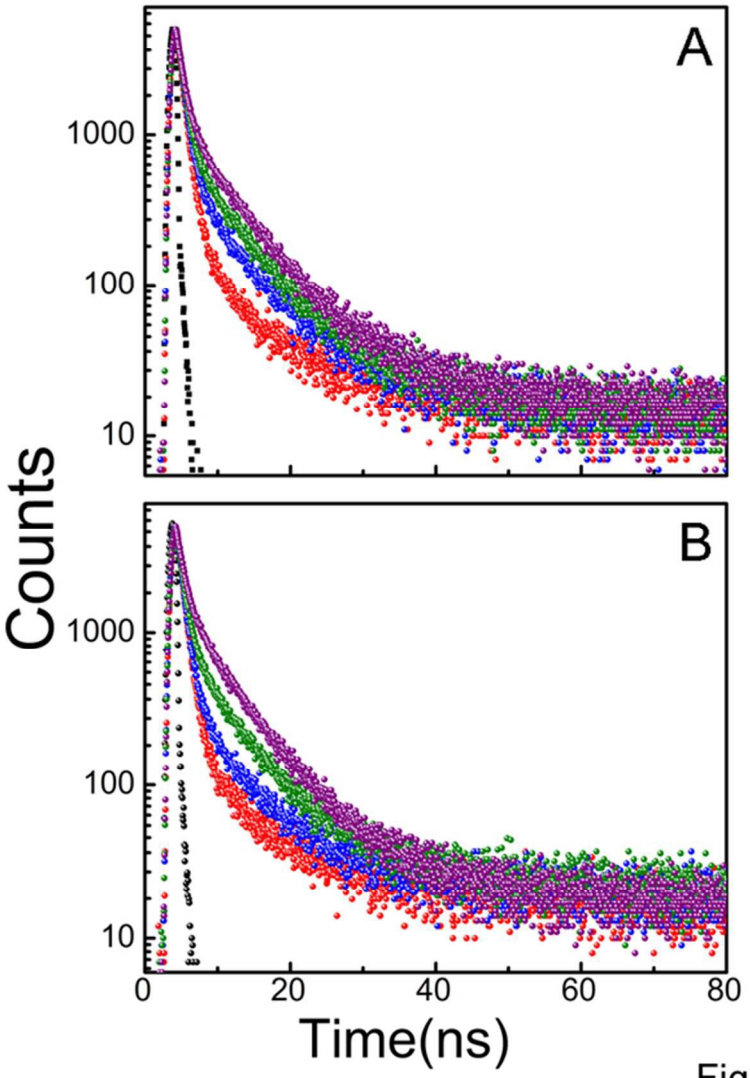

Fig. 7

55x78mm (300 x 300 DPI)

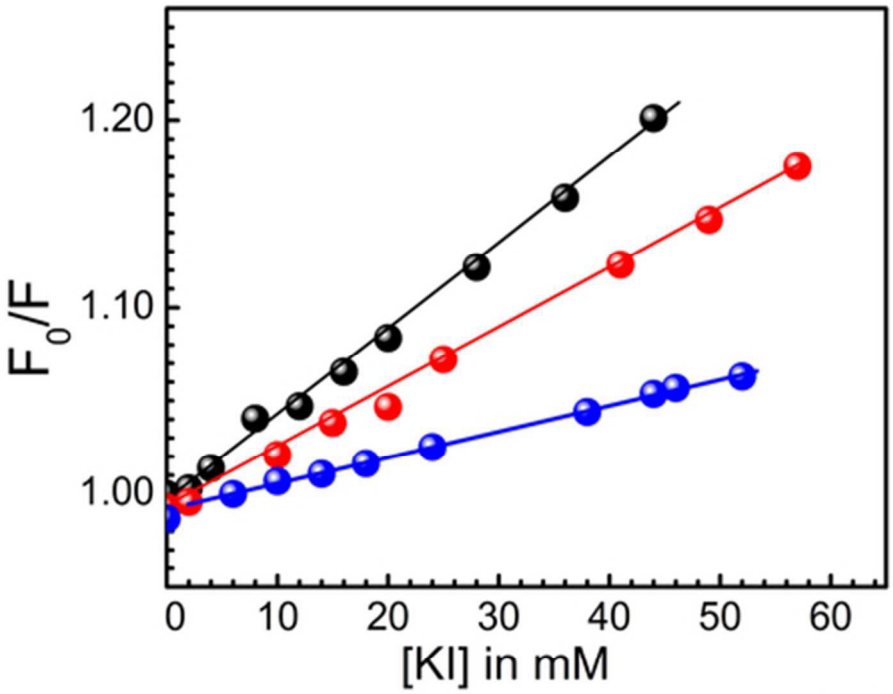

Fig. 8

40x34mm (300 x 300 DPI)

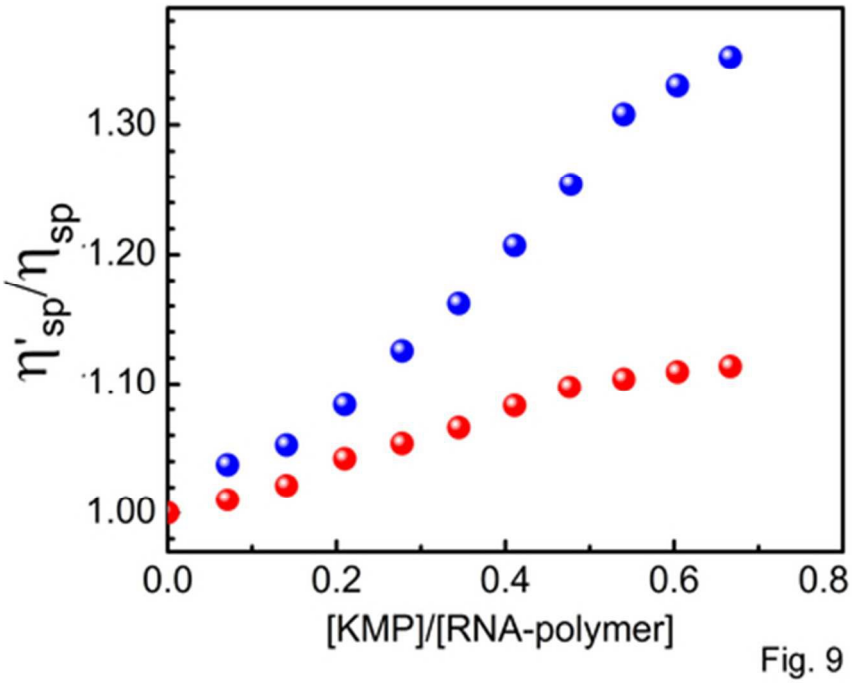

Fig. 9

39x31mm (300 x 300 DPI)

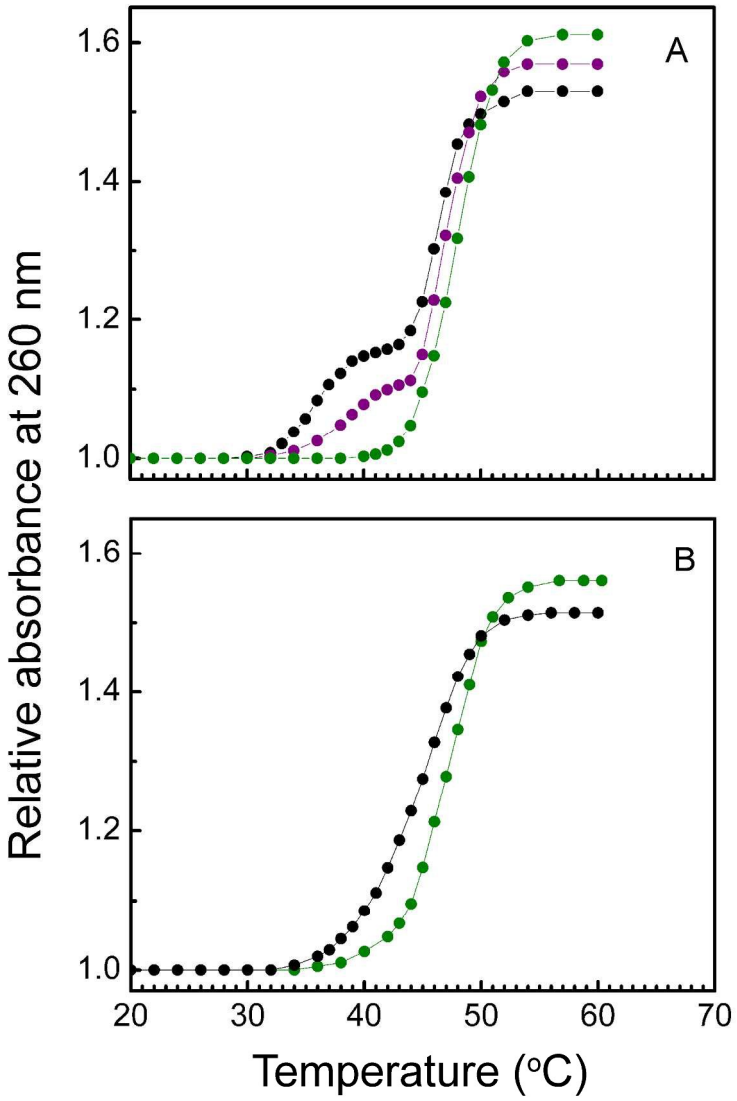

Fig. 10

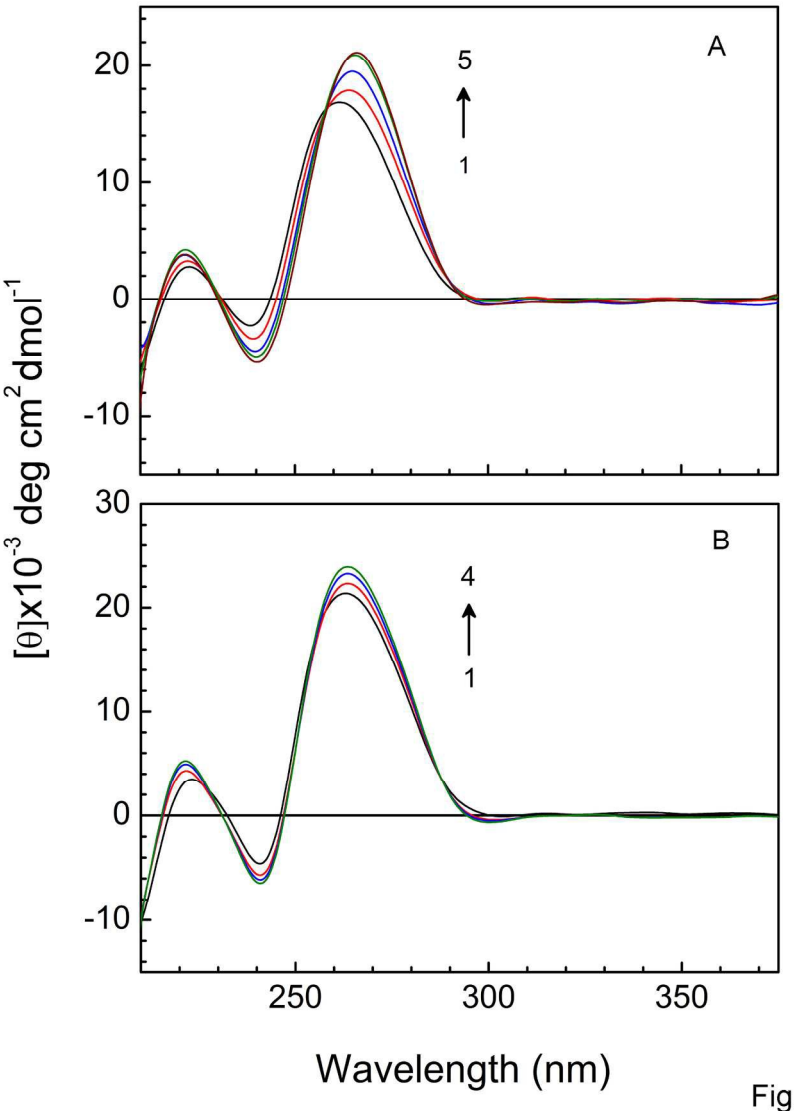

Fig. 11

168x230mm (300 x 300 DPI)

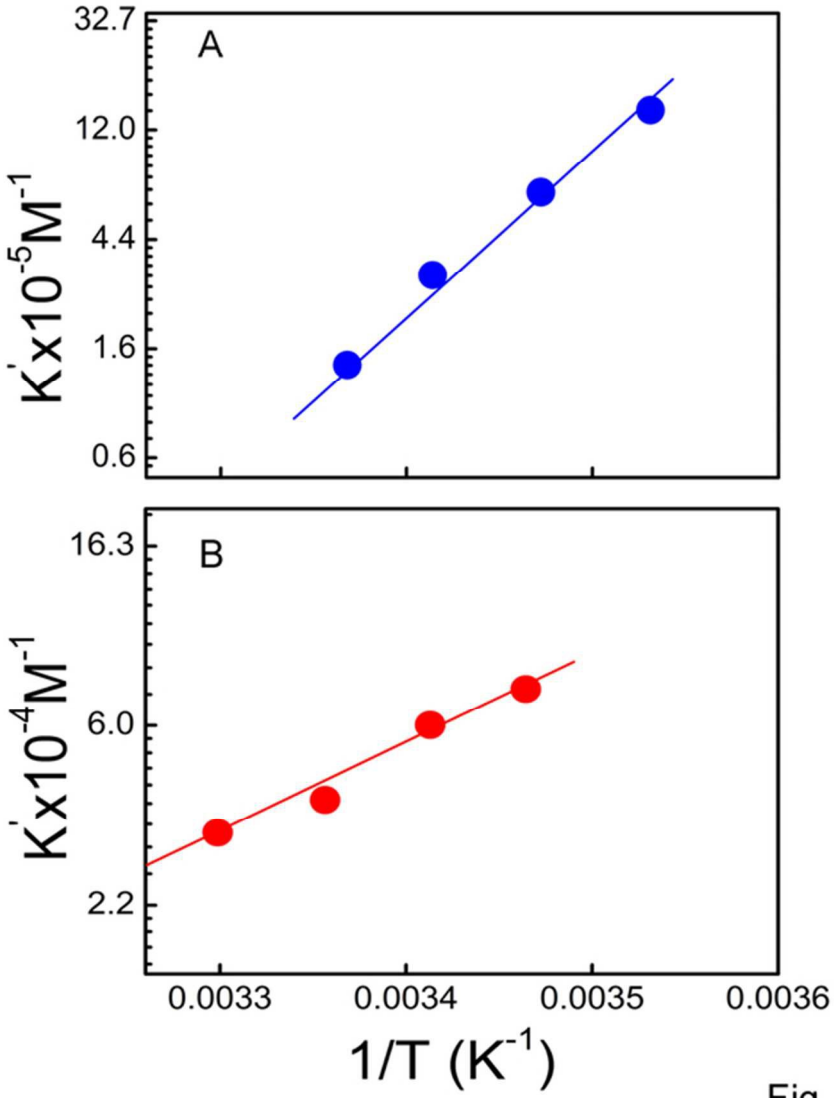

Fig. 12

55x69mm (300 x 300 DPI)

Graphical Abstract

Binding of Kaempferol with Triple and Double Helical RNA

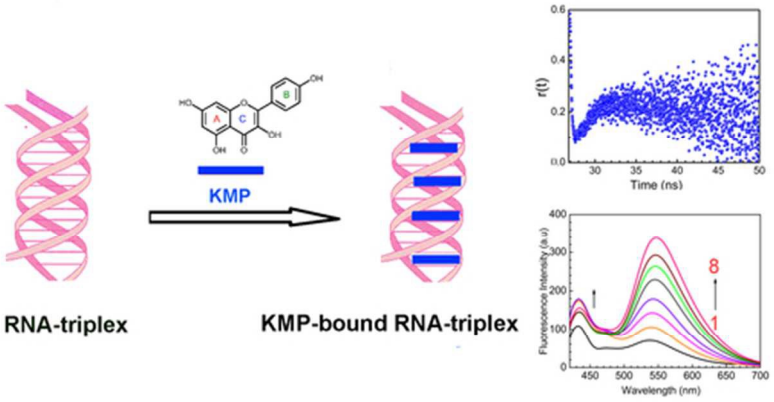

55x32mm (300 x 300 DPI)